Renewable Energy 269 (2026) 125807

Contents lists available at ScienceDirect

Renewable Energy

journal homepage: www.elsevier.com/locate/renene

Integrating classical methods and a new viability index to assess shallow ground heat exchange potential: application to the Gioia Tauro coastal plain (Calabria, southern Italy)

Giovanni Vespasiano [a,b], Marco Taussi [c,*], Luigi Russo [a,d], Giuseppe Cianflone [a,b], Lorenzo Chemeri [c], Ilaria Fuoco [a], Andrea Bloise [a,**], Mauro F. La Russa [a], Rocco Dominici [a,b], Stefania Venturi [e], Jacopo Cabassi [f], Rosanna De Rosa [a], Adriano Guido [a], Alberto Renzulli [c], Federico Ciniglia [a], Carmine Apollaro [a]

[a] Department of Biology, Ecology and Earth Sciences (DIBEST), University of Calabria, Via Ponte Bucci, Cubo 15B, 87036, Rende, Italy
[b] E3 (Earth, Environment, Engineering) Soc. Coop. and Spin-Off of University of Calabria, Via Ponte Bucci, Cubo 15B, 87036, Rende, Italy
[c] Department of Pure and Applied Sciences, University of Urbino Carlo Bo, Via Ca' Le Suore 2/4, 61029, Urbino, Italy
[d] Institute on Membrane Technology (ITM-CNR), Rende (CS), Italy
[e] Department of Earth Sciences, University of Florence, Via G. La Pira 4, 50121, Florence, Italy
[f] Institute of Geosciences and Earth Resources (IGG), National Research Council (CNR), Via G. La Pira 4, 50121, Florence, Italy

ARTICLE INFO

Keywords:
Shallow ground heat exchange potential
Open-loop
Closed-loop
GPVI
Renewable energy
Gioia Tauro plain

ABSTRACT

This study investigates the shallow ground heat exchange capability in the highly industrialized Gioia Tauro Plain (Southern Italy), integrating geological, hydrogeological, thermal, and geochemical data to assess the feasibility of both closed-loop and open-loop systems associated to geothermal heat pumps. For closed-loops the G.POT method was applied, enabling the calculation of extractable thermal energy based on soil properties and climatic conditions. For open-loops a comprehensive analysis was conducted using aquifer transmissivity, hydraulic conductivity, and geochemical features to identify the most suitable sectors. For the latter systems, a newly developed Geothermal Potential Viability Index was also proposed for a simplified system evaluation. Results show that the north-western sector of the plain has the highest suitability for closed-loop installations, due to high thermal conductivity and shallow water table. In contrast, areas near the Mesima and Budello river mouths exhibit physicochemical limitations for open-loop use, such as calcite oversaturation, high salinity, and elevated trace metal concentrations, which may significantly reduce the efficiency of open-loop systems. This integrated assessment provides a robust tool for energy planning, helping to identify high-potential zones while accounting for environmental risks and economic constraints.

1. Introduction

The exploitation of shallow ground heat exchange represents one of the most promising solutions for heating and cooling residential, commercial, and industrial indoor air conditioning systems, which can significantly reduce the greenhouse gas emissions produced by traditional fossil-fuel-based systems [1,2]. These resources can be easily exploited in non-active geological settings and at average depths of 100 m [3,4]. The energy produced by shallow ground heat exchange has increased by 52% in the last years (2015 to 2020) at a rate of 8.73% per year [1]. Typically, the first 5-15 m of soil are strongly affected by atmospheric temperature variations, but beyond these depths the soil temperature increases according to the geothermal gradient (~30 °C/km, on a global average) and remains nearly constant where no thermal anomalies are present (e.g., batholiths, sill, magma chambers). The subsurface is thermally stable, meaning it is cooler than the atmosphere in summer and warmer in winter. These shallow systems are installed using different methods, depending on the type of heat exchange with the subsurface. A ground-source heat exchanger (GSHE; [5]) equipped with a geothermal heat pump is a common type of air

* Corresponding author.
** Corresponding author.
E-mail addresses: marco.taussi@uniurb.it (M. Taussi), andrea.bloise@unical.it (A. Bloise).

https://doi.org/10.1016/j.renene.2026.125807
Received 28 July 2025; Received in revised form 20 February 2026; Accepted 14 April 2026
Available online 22 April 2026

conditioning system that utilizes the ground both as a heat source and sink (in heating and cooling mode, respectively) [6,7]. GSHEs are often associated with vertical closed-loop systems (borehole heat exchanger, BHE) or open-loop systems (groundwater heat exchanger, GWHE, [8]). BHE systems involve the installation of a network of pipes in which a heat transfer fluid can exchange heat with the surrounding ground. In GWHE systems, on the other hand, the heat transfer fluid is usually groundwater [5,9]. Unlike GWHE, whose installation is closely linked to the hydrogeological framework of the area [10], BHE can be developed practically anywhere [4], although careful monitoring is required to ensure the longevity of the system and avoid long-term depletion of the thermal reservoir in the underground [11]. These systems, also known as "geo-exchange systems", can regenerate themself and store energy for future use in different seasons. Recently, in Italy, the installation of GSHE has increased, especially in northern regions [12], while in southern regions this solution still mainly relates to cooling during the summer period [13,14]. The installation of GSHE requires detailed knowledge of geological, hydrogeological, and thermophysical characteristics. All these characteristics are necessary to define the ground heat exchange potential of an area, which is described as the thermal energy that can be sustainably exchanged with the ground through the installation of a GSHE [15]. In this framework, the present work aims to gather and combine all these features to obtain the spatial variability of the ground heat exchange potential in the Gioia Tauro plain. The latter extend for ~240 km^2 and hosts about 160k people, being among southern Italy's most important industrialized and coastal agricultural areas. For the purposes, the Geothermal POTential method (G.POT) developed by Casasso & Sethi [15] was applied to treat BHE systems, while the methodology described by Muñoz et al. [8] was used to deal with GWHE systems, in combination with a new proposed GWHE feasibility index (Geothermal Potential Viability Index - GPVI). An evaluation of the costs associated with the installation of the GSHE was also carried out, and the physicochemical features of the local aquifer were analysed to assess the possible geochemical impact of their intensive use. The work's results help in the identification of the most suitable portions of the Gioia Tauro plain for GSHE systems, facilitating the planning of future small-scale BHE- and GWHE-based energy installations. These outcomes can encourage new investments in these climatization systems, thus providing significant environmental benefits by substantially reducing local CO_2 and particulate emissions associated with standard fossil-fuelled air conditioning systems. In addition, the proposed new index, which can be applied in different geological contexts, provides an estimation of the GWHE potential, thus representing a powerful tool for private and public entities to exploit the resource.

2. Study area and geological background

The Gioia Tauro Coastal Plain (Calabria region, southern Italy) covers ~240 km^2 and is bordered to the west by the Tyrrhenian Sea, to the north by the Capo Vaticano promontory, to the south by the Palmi High, and to the east by the Serre chain. It is crossed by the Petrace and Mesima rivers and it is the second-largest Calabrian plain after the Sibari one [16], hosting ~160k inhabitants. The land use is mainly devoted to agriculture. From a geological point of view, the Gioia Tauro plain represents an Upper Pliocene semigraben, NNE-SSW oriented [17]. The plain boundaries are marked by three main fault systems (Fig. 1a): (i) the NNE-oriented and east-dipping Cittanova normal fault (CF) along the eastern margin, (ii) the NW-oriented Nicotera-Gioiosa fault (NGFZ) along the northern margin (with transcurrent kinematics), and (iii) the NW-oriented Palmi-Locri transcurrent fault (PLFZ) to the south [18]. Additionally, three other faults parallel to the CF occur: (i) the west-dipping St. Eufemia-Laureana (SLF) normal fault that crosses the central sector of the plain, (ii) the east-dipping Palmi-Gioia Tauro high-angle fault (PGF), near the coast, and the west-dipping Rosarno--Palmi fault (RPF) [19]. The Serre Massif outcrops along the eastern boundary of the plain and consists of metamorphic and plutonic Varisican rocks [19,20] covered by Neogene-Quaternary sedimentary successions [21,22]. To the south of the area, the PLFZ separates the Serre Massif from the Aspromonte Massif [20], which consists of medium-to-high-grade metamorphic rocks that outcrop in the Petrace river basin. The southwestern side of the plain is bounded by the Palmi High, which is characterized by crystalline rocks (migmatitic paragneisses, foliated tonalites, and gneisses) overlain by Tortonian-Messinian silicoclastic and carbonate deposits [20]. Another structural high, approximately N-S oriented, is present along the western sector of the plain near the coast [22,23]. The sedimentary fill begins with an Upper Miocene carbonate and silicoclastic succession (mainly outcropping along the Palmi High), which discordantly overlies the crystalline basement. Upward, the succession passes to the "Trubi Formation", consisting of Pliocene clay and silty deposits [21,24]. The infill continues with "Vinco Calcarenites", consisting of sands and late Pliocene-Pleistocene calcarenites. The alluvial conoid deposits of the "Taurianova Synthema" (Late Pleistocene) overlie the Vinco Calcarenites along an erosional contact [18]. The sedimentary fill of the plain ends with Pleistocene-Holocene terraced marine deposits (sand and gravel up to 20 m thick). In the Gioia Tauro Plain, three main hydrogeological units were recognized [18]: (i) the shallow unconfined aquifer, which contains all Quaternary successions (HU3); (ii) the aquitard, consisting of Pliocene clay and silt deposits of the Trubi Formation (HU2); (iii) the deep aquifer, consisting of Upper Miocene clastic and limestone deposits (HU1) (Fig. 1b and c). The presence of deeper water circuits within the crystalline basement is indicated by the Galatro hot springs [25,26].

3. Materials and methods

3.1. Ground heat exchange potential estimation

The methodological approach represents an evolution of that proposed by Ondreka et al. [28] and already applied in several works [29–31]. The approach involves: i) collection of geological, stratigraphic, hydrogeological, thermophysical, climatic, and economic data of the area of interest; ii) data elaboration and creation of iso-distribution maps and iii) evaluation of the ground heat exchange potential for both BHE and GWHE. For the GWHE, some of the physical-chemical conditions of the aquifer were investigated to predict possible criticalities associated with intensive exploitation. Furthermore, a new index (GPVI) was introduced to simplify and enhance decision-making. All data were collected and organized at the investigated area scale (Fig. 1). A reference thickness of 100 m was chosen, since it is the most common depth involved in vertical heat exchange systems. Since the analyses of semi-variogram models describing the spatial dependence of the investigated variables reported a purely nugget effect, the deterministic inverse distance weighted (IDW) interpolation was used to produce the spatial distribution maps.

3.1.1. Lithostratigraphic and hydrogeological data

For the subsoil reconstruction, data from 257 wells, derived from ISPRA [27] database, were elaborated. Each well was partitioned into homogeneous, saturated or unsaturated layers, according to the depth of the aquifer. Each layer was associated with a specific category derived from the soil classifications used in the Italian Seismic Microzonation studies, following the modified "Unified Soil Classification System" [32]. This process was necessary to homogenise the data under a single guideline and simplify the treatment of the different lithologies in the territory. The various soil types were classified (based on the dominant grain size) as gravel, sand, clay, or silt. Hydrogeological characteristics of the aquifers (saturation depths and piezometry) were also defined since they are crucial factors for the evaluation of the heat exchange potential [33]. To standardise the data, stratigraphical information below 100 m of depth were not considered. In contrast, wells with shallower depths were virtually extended, considering homogenous

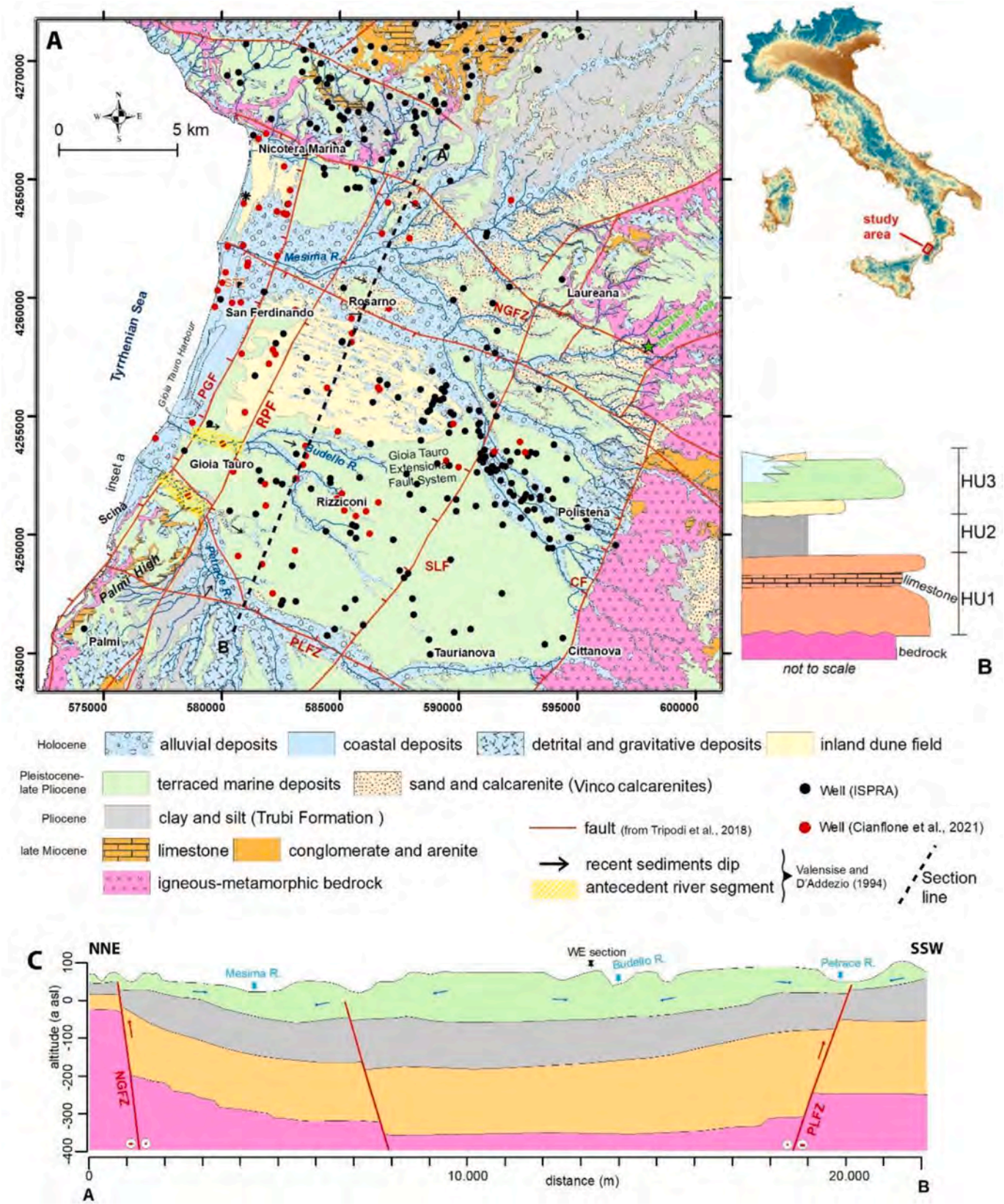

Fig. 1. (a) Geological map of the Gioia Tauro plain (modified from Vespasiano et al., [19]). The map shows the wells used for ground heat exchange potential estimation purposes collected from ISPRA [27], Cianflone et al., [23] and Vespasiano et al., [19]. (b) schematic stratigraphic column (not to scale) and N-S hydrogeological section showing the deep (HU1) and shallow (HU3) aquifers and the aquitard (HU2) recognized in the study area. **NGFZ**: Nicotera-Gioiosa fault; **PLFZ**: Palmi-Locri fault; **CF**: Cittanova Fault; **SLF**: St. Eufemia-Laureana fault; **PGF**: Palmi-Gioia Tauro high-angle fault; **RPF**: Rosarno-Palmi fault.

lithostratigraphic features to bring the last horizon up to the required depth. To maintain proper assumptions on the stratigraphical data we used nearby deep wells' stratigraphy and geological cross-sections (e.g., Fig. 1c).

3.1.2. Thermophysical properties of the underground and ground heat exchange estimation

The Specific Heat Extraction rate (SHE, in W/m) of the subsoil provides the value of extractable power per unit length for different lithologies. To calculate the SHE of each well, it was firstly necessary to assign to each lithology a tabulated value concerning (i) the specific thermal conductivity (λ, in W/mK) reported in the literature for the Calabria Region main lithologies [34] and for unconsolidated materials [35,36], and the (ii) volumetric heat capacity (ρC, in MJ/m^{3}K) [37], which allow to understand the heat transfer capacity of the subsurface and, consequently, to ensure efficient heat transfer of the system (used values are in Table S1 [38]). The highest values of these properties are attributed to the saturated horizons and bedrock, where heat is exchanged with greater efficiency. The SHE was calculated for each lithology following the relationship reported by Viesi et al. [4]. The detailed procedure is reported in the Supplementary Material.

The amount of heat that can be exchanged with the subsurface was estimated using the G.POT (Geothermal POTential) method [15] and was calculated based on the thermal need of a standard residential house of 100 m^2 (i.e., 5 kW; see Supplementary Material). The G.POT allows the calculation of the Q_{BHE} for each well (in MWh/y), defined as the average heat load that can be sustainably exchanged between the BHE system and the subsoil per unit of time, avoiding significant thermal impact on the ground. This approach involves several variables related to (i) thermal properties of the soil (λ, ρC, and undisturbed soil temperature T_0, in Kelvin); (ii) BHE properties such as depth (L in meters), borehole radius (r_b in meters), and thermal resistance (R_b in mK/W); (iii) system properties such as minimum fluid temperature during the heating mode, climatic conditions, and operating life. While some of these parameters are standardized and commonly used for this type of calculation, some others are dimensionless or experimentally evaluated. The values used in this work are reported in Table S2 [38] and detailed in the Supplementary Material.

3.1.3. Economic cost estimation

If compared with other systems, the costs for the BHE installation are usually higher due to the drilling of the vertical boreholes. For this reason, we focused on estimating the drilling costs considering the power demand of 5 kW. The cost analysis was based on the price list of public buildings made by the Calabria Region (https://www.regione.calabria.it/). Non-coring drilling was considered with its different costs depending on the crossed lithotype (sedimentary infill or crystalline bedrock) and depth (greater or lesser than 30 m) (Table 1). To prevent hole instability that may take place during drillings, a provisional coating can be installed, raising the costs. For drilling in the sedimentary infill and crystalline bedrock, the use of provisional coatings was evaluated for both the entire hole length and then only for the segment under the water table. An additional cost for the equipment transport and drilling site preparation should be added to the drillings' prices.

Table 1
Costs (€/m) of non-coring drilling and provisional coating (obtained from the price list of the Calabria Region).

Drilled lithotype	Non-coring drilling cost (€/m)		Provisional coatings cost (€/m)	
	depth <30m	*depth >30m*	*depth <10m*	*depth >10m*
Sedimentary infill	40.6	49.8	12.2	16.8
Crystalline bedrock	49.8	59		

3.2. Open-loop system

Open-loop systems work by extracting heat usually from pumped groundwater, which is transferred to the heat pump, and then typically re-injected into the aquifer or in surface waters or in sewage network [39]. The potential for the exploitation of open-loop systems was estimated using the approach of Muñoz et al. [8]. For this purpose, a regular network of points (750 × 750m) was constructed to which the values of the required hydrogeological parameters were assigned.

3.2.1. Hydrodynamic properties of the aquifer

Hydrodynamic properties allow the estimation of the expected lowering of the groundwater level (because of the pumping by the GWHE) and concern transmissivity (T, in m^2/s) and hydraulic conductivity (K, in m/s). The adopted approach follows Logan [40]. The hydraulic properties of each investigated well were estimated through flow rate (Q, in m^3/s), static level, thickness of the aquifer (m) and its lowering (S_w). Accordingly, T and K were estimated as:

$$\boldsymbol{T} = (\mathbf{2.46} \cdot \boldsymbol{Q} \cdot \boldsymbol{m}) \,/\, \boldsymbol{S_w}\,(\mathbf{2}\boldsymbol{m} - \boldsymbol{S_w}) \quad (1)$$

$$\boldsymbol{K} = \boldsymbol{T}/\boldsymbol{m} \quad (2)$$

To simplify the data treatment, the approach regarded only the shallow aquifer so, below the piezometric level, the whole well was considered in saturated conditions. This assumption is justified by the observed grain size consisting of sands and conglomerates with high K. In absence of specific data, the intercepted portions of the crystalline basement were treated as unsaturated. Detailed values are reported in Table S3 [38].

3.2.2. Output and excavation depth

The excavation depth for open-loop systems was evaluated by calculating the Q of the GWHE system, as shown in eq. (3) which depends on the: (i) energy required by the building (P, in J/s); (ii) groundwater's density (ρ, in kg/m^3) and specific heat capacity (Cp, in J/kgK); (iii) temperature difference between the water entering and leaving the heat pump (ΔT, in °C):

$$\boldsymbol{Q} = \boldsymbol{P}/\,(\rho \cdot \boldsymbol{Cp} \cdot \Delta\boldsymbol{T}) \quad (3)$$

The thermal need for a standard-sized residential house of 100 m^2 was considered also in this case equal to 5 kW. The ΔT was set at 6 °C [36] as some authors [41,42] demonstrated that exceeding an average of 20 °C can lead to microbial alteration and geochemical activity in the aquifer. For this reason, the calculations were made considering ΔT from the aquifer's undisturbed temperature of 3, 4, 5, and 6 °C. S_w and excavation depths, both expressed in meters, were calculated as follows:

$$\boldsymbol{S_w} = \sqrt{(\mathbf{2} \cdot \boldsymbol{Q})\,/\boldsymbol{K}} \quad (4)$$

$$\mathbf{GWHE_{depth}} = \mathbf{2} \cdot (\text{static level}) + \mathbf{S_w} \quad (5)$$

3.2.3. Geochemical issues associated with the open-loop systems

The groundwater's chemical characteristics exploited by open-loop systems can create some problems in the used components and may involve an imbalance in the physico-chemical conditions of the aquifer [42]. Thus, it is paramount to study the potential geochemical issues that may occur, to prevent major economic expenses for the construction and maintenance of a GWHE. These problems may include: i) aggressiveness of the water towards the system's components [43]; ii) clogging of the circuits due to precipitation of saturated mineralogical phases [43], and iii) increase in proliferation of bacteria potentially harmful to human health [41,43]. Previous geochemical data [19,23] collected at the Gioia Tauro plain were elaborated to assess potential chemical impacts related to the use of open-loop systems. We defined the saturation state of the main mineralogical phases to assess possible scaling effects

in the system's piping. Furthermore, due to the disturbances induced by the re-injection of water into the aquifer at different temperatures (higher in summer and lower in winter), we hypothesized increments or decrements in the saturation indexes (SI). To do this, based on the physico-chemical properties of the aquifer, the SI of calcite, chalcedony and gypsum (following [19]) were calculated using PHREEQC interactive software, version 3.1.1 [44], and the LLNL thermodynamic database. The calculations were performed considering the undisturbed temperature with a ΔT of ±6 °C (according to Ref. [36]).

3.2.4. Geothermal Potential Viability Index (GPVI) for open-loop system

The new *Geothermal Potential Viability Index* (GPVI) was developed and computed to expeditiously evaluate the feasibility of GWHE systems based on the main hydrological (e.g., water level, hydraulic conductivity) and geochemical (e.g., electrical conductivity EC, pH) features of an aquifer. Indeed, the assessment of the exploitation potential for GWHE must consider several factors that impact both system costs and operational management, like water table depth and temperature, K, and the physico-chemical characteristics of the groundwater. The simultaneous evaluation of these parameters entails the generation of a substantial number of thematic and value-based maps, making the overall process rather complex. The GPVI was developed to integrate these variables into a single potential value, that summarizes the overall characteristics of the aquifer by indicating whether favourable/unfavourable conditions for the implementation of a GWHE system occur, thereby facilitating land-use planning and system design. The computation of the GPVI follows the same fundamentals and principles deployed for defining the Chemical Water Quality Index (CWQI) [45], and it is divided into three steps: (i) selection and parameterization of the variables of interest; (ii) weightage and (iii) index computation.

The first step involves the selection of the variables of interest and, since they are reported in different scales, a parametrization (or transformation) phase is required [45]. The parametrization consists in assigning a score (*s*) from ~1 to 10 to each variable based on the measured value (or concentration) with respect to a reference target, carefully chosen depending on the specific variable. The reference target should represent the "maximum allowable value for having favourable conditions for implementing a GWHE system" (see Table 2). The "*score-assigning function*" (eq. (6)) was developed following the U-Richards sigmoid equation [45] where *x* represents the input value, *a* is the upper asymptote (set equal to 10), and the three unknown parameters (*b*, *c* and *d*) are determined for each variable through a least squares iterative procedure for finding the best-fitting curve to the given set of points (Table 2). The fitting curve was forced to pass through (1; 5) (full details are reported in Ref. [45]):

$$s_x = a^* \left(1 + (d-1)^* exp \left(\frac{-b^*(x-c)}{d^{\left(\frac{d}{1-d}\right)}} \right) \right)^{\frac{1}{1-d}} \quad (6)$$

Variables' choice is at user's discerption; however, we suggest to consider the following: EC, pH, K, water level, temperature (expressed as ΔT and indicating the temperature seasonal variability), redox potential (Eh), SI for calcite ($CaCO_3$), gypsum ($CaSO_4$) and chalcedony (SiO_2), and the elemental concentrations of Fe, Mn. The parameters *a*, *b*, *c* and *d* for each variable are reported in Table 2.

Depending on the selected variable, the input value (*x*) must be calculated as follows:

(1) measured value/reference value;
(2) the value of K should be transformed as follows: -log($K_{measured}$)/-log($K_{reference}$);
(3) SI_x should be transformed in the saturation state (10^{SI}): $10^{SI\ (measured)}/10^{SI(reference)}$;
(4) For parameters such as pH and Eh for which the ideal value is represented by a range of values, the input value should be calculated as follows (eq. (7)):

$$\Delta x = \frac{\left|\overline{x}_{ideal} - x_{measured}\right|}{|x_{max} - x_{min}|} * 2 \quad (7)$$

where x_{max} and x_{min} represent the maximum and minimum admissible value, respectively, and $\overline{x}_{ideal}$ represents the barycentre of the range (i.e., the ideal value) given by the arithmetic mean between x_{max} and x_{min}.

In addition, for reasons of practical feasibility, the implementation of a GWHE is not feasible for depth to water table <2 m, while when <5 m it is necessary to evaluate the individual case study. Eventually, when the concentrations of the considered elements are below the detection limit (DL), the DL/2 value should be reported for calculating the GPVI [45].

Each parameter was selected based on specific considerations. EC maximum value was set at 2250 μS/cm following the salinity hazard of irrigation water in terms of sodium adsorption ratio (SAR) [46]. The ΔT was prudentially maintained half of the maximum value of 6 °C, thus avoiding risk of alteration of the microbial and geochemical activity of the aquifer. K was considered optimal when $>10^{-5}$ m/s, which is the typical value of gravelly-sandy aquifers, able to permit a high flow rate both for extraction and reinjection [47,48]. Maximum and minimum water levels were set at 50 and 2 m, respectively. The deeper one represents the depth after which the economic benefits of installing a GWHE drop, and the costs overpass those of installing a BHE, while the lowest represents a depth that could avoid an excessive increase of the water table during re-injection operations. SI threshold values were set at 0.5, considering a slightly supersaturated state that would prevent clogging issues. Ideal values of pH range from 6 to 8, i.e., reflecting circumneutral conditions, while positive Eh values were considered as ideal, since they would inhibit metals mobility. Finally, concentrations of ionic metals were evaluated with respect to the quality targets provided by the European Union legislation for drinking waters [49].

Following the parametrization step, the weight (*w*), directly proportional to the score (*S*), is assigned to each parameter following:

$$w_x = \frac{S_x}{\sum_{i=1}^{n} S_i} \quad (8)$$

Table 2
Values of the unknown parameters *a, b, c* and *d* calculated for each variable. The reference value, input value and the bibliographic reference for each variable are also reported.

Variable	a	b	c	d	Reference value	Input	According to
EC	10.00	0.46	0.60	0.78	2250 μS/cm	1	[46]
ΔT	10.00	0.48	0.82	1.29	3.0 °C	1	[36]
K	10.00	0.47	0.65	0.85	10^{-5} m/s	2	[47,48]
Water level	10.00	0.51	0.85	1.36	50 m	1	*Half of the required depth for the BHE*
SI_x	10.00	0.52	0.68	0.84	0.5	3	[43]
pH, Eh	10.00	0.58	0.56	0.53	6.00-8.00 (pH) 0-200 meV (Eh)	4	[43]
Concentrations	10.00	0.54	0.70	0.88	Potability limits	1	*Threshold value according to* [49]

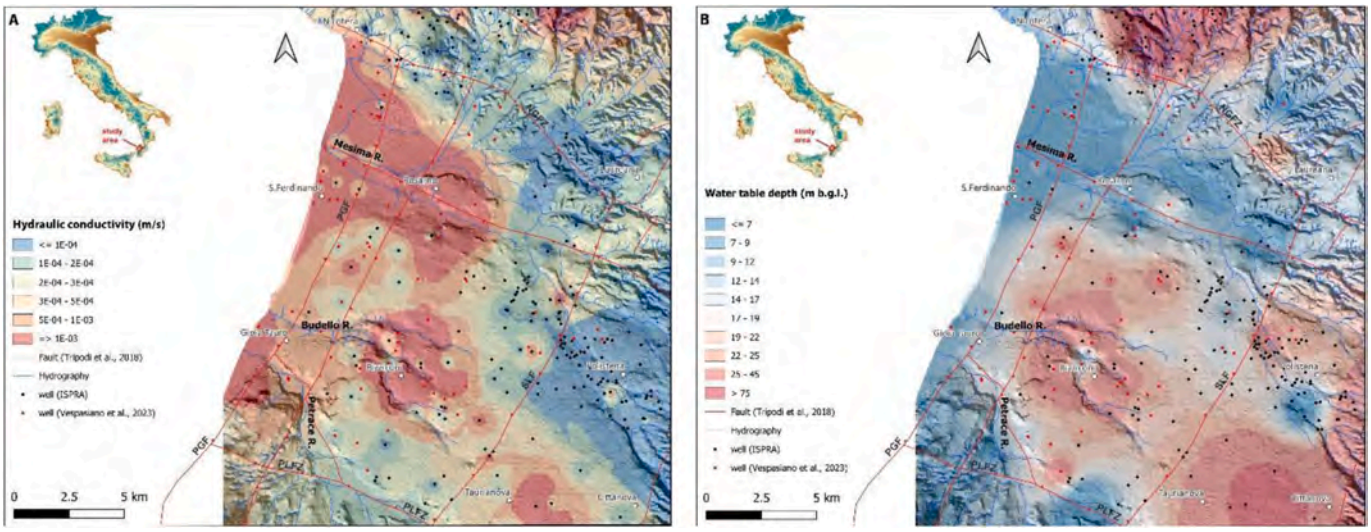

Fig. 2. Maps of the (a) hydraulic conductivity (K) and (b) water table depth of the Gioia Tauro plain.

where w_x indicates the weight of the parameter x, S_x is the score computed for the parameter x and $\sum_{i=1}^{n} S_i$ represents the sum of the scores of all the n parameters considered [45]. This formulation gives at each variable a relative importance that only depends on the measured value and the corresponding reference, meaning that the weights are not determined *a priori* but are evaluated every time a new water sample is tested [45].

The final step involves the index computation in which the single scores and weights are aggregated together, producing a single value summarizing the aquifer's favourability/unfavorability. The GPVI uses a weighted geometric average, since a multiplicative aggregation produces more reliable results and reduces possible eclipsing problems [45]. The GPVI index is computed as follows:

$$GPVI = \prod_{i=1}^{n} S_i^{W_i} \tag{9}$$

The calculated GPVI will vary from ~1 to 10, with lower values corresponding to favourable conditions for implementing a GWHE system with increasingly unfavourable conditions as the value increases.

For the GPVI determination we recommend to carry out a two-step calculation: first, conduct an exploratory analysis by considering only pH, temperature, EC, water level and K, i.e., the most relevant parameters from an engineering feasibility point of view and the easier to determine (*simplified*-GPVI). Consequently, for values < 5 (i.e., favourable-to-boundary conditions), it is recommended to expand the number of variables considered towards a better characterization of the aquifer, focusing on water chemistry (Table 2), by computing a *detailed*-GPVI. The outcomes of the GPVI can be classified into 6 condition categories: (1) optimal (<2.00), (2) very good (2.01<GPVI<4.00), (3) boundary (4.01<GPVI<5.00), (4) likely unfavourable (5.01<GPVI<6.00), (5) unfavourable (6.01<GPVI<8.00), and (6) very unfavourable (>8.00). The accuracy of the outcomes for this approach was tested and confirmed in Chemeri et al. [45]. A limitation for the index may be represented by those aquifers characterized by a limited number of parameters that strongly exceed the reference value. In these cases, the GPVI may be overestimated [45].

4. Results and discussion

4.1. Hydro-stratigraphic and hydrodynamic reconstruction

The distribution of K and water table depths for the HU3 (Fig. 1b) hydrogeological unit, the one of greatest interest for the calculation of

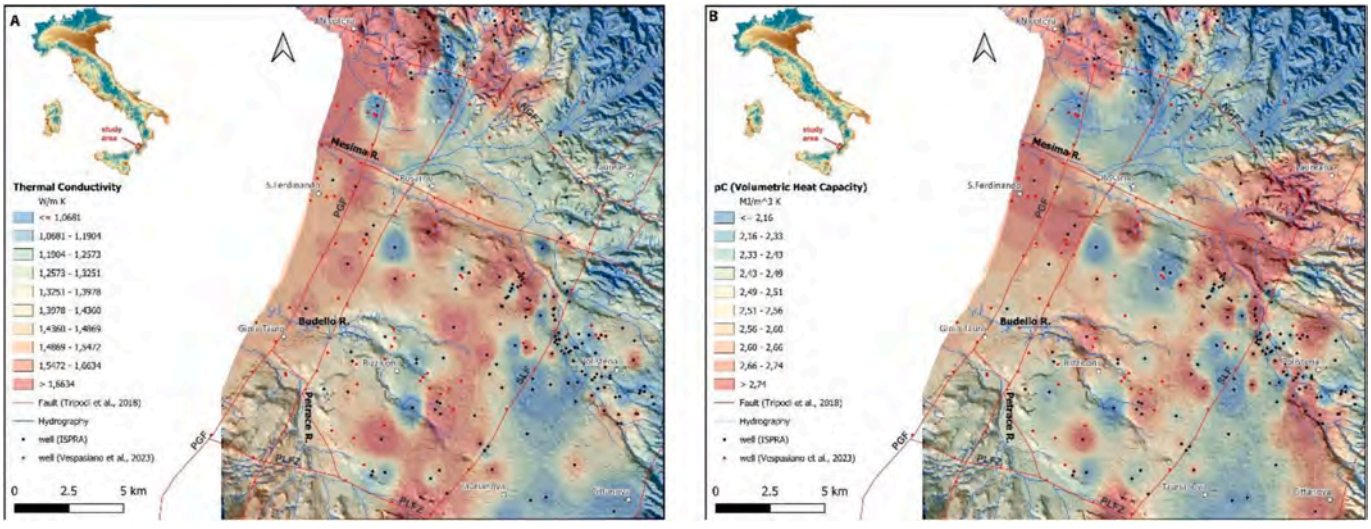

Fig. 3. Maps of the (a) thermal conductivity (λ) and (b) volumetric heat capacity (ρC) of the Gioia Tauro plain.

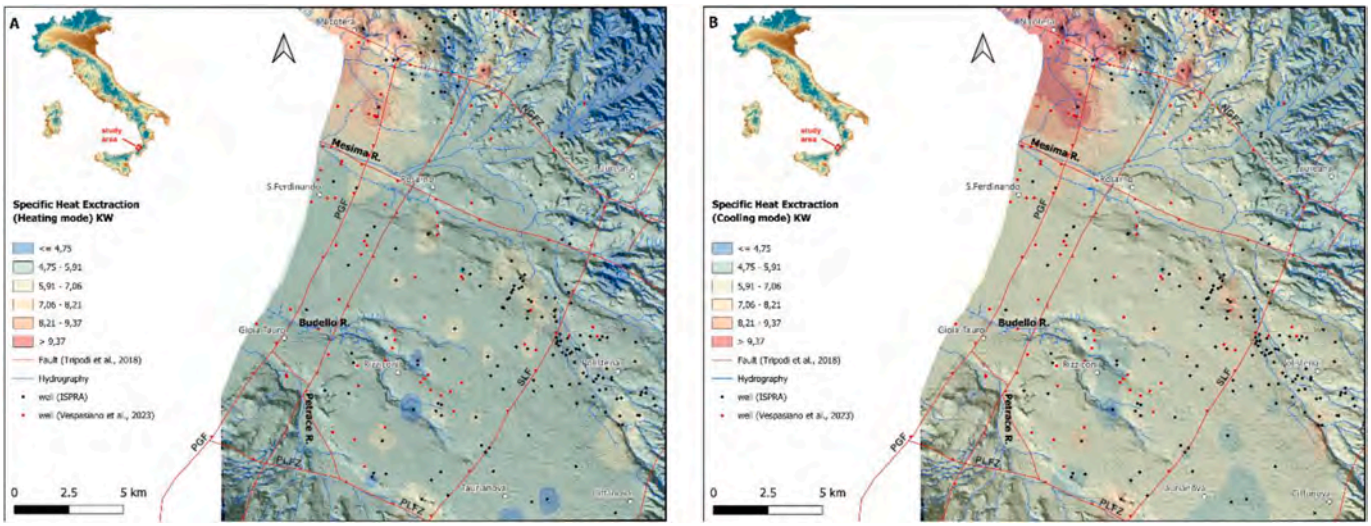

Fig. 4. Heat extraction values of the Gioia Tauro plain for a) heating and b) cooling mode.

shallow heat exchange capacity, are shown in Fig. 2.

The sectors with lower K are in the innermost portions of the plain at higher elevations and where the crystalline basement and clayey successions approximate the surface. These areas also correspond to the deepest groundwater levels. On the other hand, the more permeable areas (with the lowest groundwater levels) are localized toward the coastline characterized by the coarsest Pleistocene deposits. The K of the coastal plain is generally high, ranging from 6.9×10^{-5} to 2.4×10^{-3} (m/s). The maximum values are found in the western-central portion, due to the presence of alluvial deposits and sands, while the lowest values are found in the eastern-central area, where the Pliocene clays reach the surface, considerably reducing K. The aquifer depth ranges between <1 and 123 m below the surface. The highest values are in the northern part of the study area, where the bedrock morphology shows very high slopes, and to the southeast, where the presence of three relative highs causes the lowering of the groundwater level. The alluvial and coastal deposits reach the lowest values along the western area.

4.2. Closed-loop systems potential

The most suitable sectors of the Gioia Tauro plain for the installation of BHE plants are shown in the distribution maps of the λ and ρC (Fig. 3). Thermal conductivity values are between 0.80 and 2.88 W/mK with the highest values found in the north-western part of the study area (where the crystalline basement outcrops) and in the central portion (where the water table approach the surface). The minimum values, on the other hand, can be found in the eastern part of the study area, where the water table is deeper. The ρC values are relatively homogeneous, ranging from 1.91 to 3.02 MJ/m^3, with maximum values located in the central and eastern parts of the area, again influenced by the presence of saturated deposits, whereas the minimum values are localised in the north-eastern sector of the study area.

SHE maps (Fig. 4) were made by considering both data for winter and summer seasons (heating and cooling mode, respectively). As expected, SHE is dependent on λ. The Gioia Tauro coastal plain shows values of heat extraction from a single BHE between 4.7 and 11.01 kW for cooling mode, and between 4.14 and 9.45 kW for heating mode. The highest heat extraction values are recognized in the north-western sector of the study area, in accordance with the maximum values of λ and the presence of crystalline basement outcrops. The maps for the heating and cooling modes show comparable distribution of values, with higher average for the cooling mode due to the lower number of operating

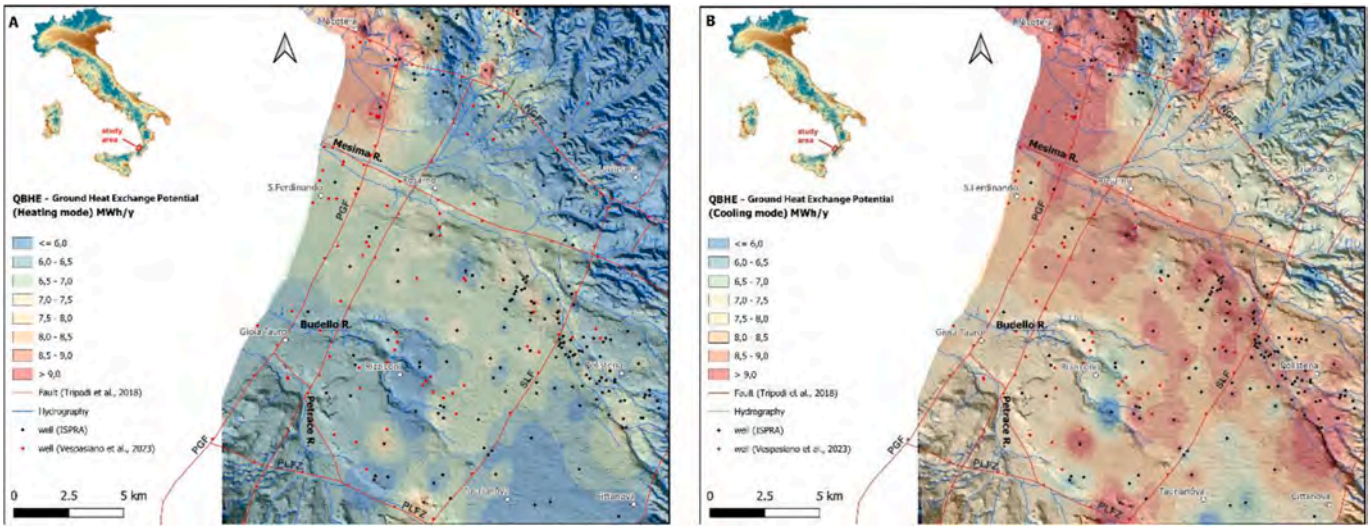

Fig. 5. Maps of estimated ground heat exchange potential of the Gioia Tauro plain obtained by applying the G.POT method relative to the (a) heating and (b) cooling modes.

hours of the plant.

The G.POT maps (Fig. 5) suggest that the highest capacity to exchange heat from the ground, both during summer and winter, is found in the north-western and central portions of the area. The maps show that between 3.65 and 9.17 MWh/y of energy can be extracted from the subsurface for heating (average: 6.41 MWh/y) and between 4.83 and 13.94 MWh/y for cooling (average: 7.98 MWh/y). Overall, the potential is controlled mainly by the λ of the lithotypes and the hydrogeological conditions, considering that ρC values are essentially constant throughout the area. The average potential estimated for heating of the Gioia Tauro plain can be considered as medium potential, compared to other areas where the G.POT has been applied in Northern [9], Central [29,30] and Southern Italy [31], or in Southern Spain [14]. For cooling potential, the average value of ~8 MWh/y is perfectly in line with studies conducted where summer demand is often prevalent [14,31]. The comparison highlights how the thermal conductivity of local lithotypes and the water table depth are the main controlling factors. In summary, the Gioia Tauro data validate the regional model, placing it coherently within the current scientific landscape for shallow ground heat exchange.

To effectively link the ground heat exchange potential to possible final users, we realized a comparison between the spatial distributions of Q_{BHE}, for both heating and cooling modes, and the resident local population (https://www.istat.it/notizia/statistiche-sulla-popolazione-per-griglia-regolare/). The Q_{BHE} was divided into four classes: (i) low (<6 MWh/y); (ii) medium (between 6 and 7.5 MWh/y); (iii) high (between 7.5 and 9 MWh/y); (iv) very high (>9 MWh/y). For each class the total population has been counted (Table 3). Referring to the heating mode: 36,044, 73,024, 5732 and 1691 persons live in low, medium, medium-high and high Q_{BHE} classes, respectively. Considering the cooling mode: 1229, 22,024, 83,496 and 9742 people live in low, medium, high, and very high Q_{BHE} classes respectively.

Considering the depth required to supply 5 kW of thermal energy for both heating and cooling modes (Table S2 in Ref. [38]), the cost for non-coring drilling (including the provisional coatings ones), was analysed. Referring to the heating mode, the minimum drilling cost of ~2800€ was estimated in the north-western sector (Fig. 6), where the depth required to supply 5 kW is lower due to the presence of the crystalline bedrock. The short length of the drilling, in addition to the unnecessary provisional coatings above the water table, allows for maintaining a low cost despite the higher cost of drilling the crystalline rocks. Between ~4500 and ~5500€ are necessary in the central and eastern sectors, where the shallow water table allows keeping low the depth required to supply 5 kW (Fig. 6). The maximum cost (>7500€) is instead calculated in the north-eastern sector (Fig. 6) due to the higher depth to be reached due to the presence of thick sedimentary infill (Fig. 1) and deep piezometric level (Fig. 2b). Regarding the cooling mode, the spatial distribution of the drilling costs is the same as that of the heating mode, but with general lower values, between 1863 and 7674€, due to the lower depth required to supply 5 kW of thermal energy. Given the reversibility of the geothermal probes that can be used in both heating and cooling modes, the costs that should be considered are those related to the deepest drillings (Heating mode; Fig. 6).

Table 3
Comparison between the ground heat exchange potential (Q_{BHE}) and the population living in the study area.

Q_{BHE}	MWh/y	Population (n. of inhabitants)	
		Heating mode	Cooling mode
Low	<6	36,044	1229
Medium	6 - 7.5	73,024	22,024
High	7.5 - 9	5732	83,496
Very high	>9	1691	9742

4.3. Open-loop systems potential

Fig. 7a highlights the most suitable areas of the Gioia Tauro plain for the installation of GWHE. The results refer to a standard energy demand of 5 kW and a temperature range variation of 6 °C. The property that most influences the yield of an open-loop system is K (Fig. 2a). The excavation depths (Fig. 7a) required to match the thermal energy supply are between ~4 and 250 m. The minimum and maximum depths can be found in the north-central and north-western sectors, respectively. The risk of lowering the aquifer level, induced by the exploitation of groundwater, appears to be low (maximum drawdown 0.81 m), and depends on the generally high K of the soils. The areas where the K is lower (characterized by the presence of clay and silty soils) show a greater lowering-risk of the water table. On the other hand, the more permeable portions represented by sands or conglomerate deposits are characterized by a rapid hydraulic recharge of the system and, consequently, by a lesser lowering risk of the water table. These results are consistent with the findings of Casasso and Sethi [9] and Muñoz et al. [8] since in both cases the technical feasibility of GWHEs is primarily governed by local hydrogeological parameters, such as aquifer T and water table depth. Eventually, the estimated drilling costs for GWHE implementation show values ranging from <1000 to 15,646€, strongly depending on the depth of the saturated level (Fig. 7b).

4.3.1. Geochemical issues associated with the open-loop systems

Groundwater chemical characteristics play a key role in the economic evaluation of a GWHE system, as it may have corrosive or encrusting properties that could reduce the plant's efficiency. The chemical and physical properties of the aquifer and the SI of the main mineralogical phases were analysed and mapped to identify the most suitable areas for the installation of GWHE systems.

The saturation state of each water sample was calculated by considering both the undisturbed aquifer temperatures (Fig. 8) and using a ΔT of ±6 °C but constraining the chemical composition of the solution.

All the analysed waters exhibited undersaturation with respect to gypsum, both at the aquifer's undisturbed temperature and under simulated conditions with a ±6 °C temperature variation (*not show*). This suggests that sulphate and calcium concentrations are unlikely to represent limiting factors for the open-loop systems' operativity. Conversely, SI for calcite ranged from −2.5 to >+0.5, allowing the identification of critical areas prone to precipitation and scaling, recognized at the northern sector, the mouth of the Mesima river, and the Palmi High southwards to the Budello river mouth. Oversaturation becomes more pronounced under higher temperature scenarios (+6 °C; Fig. 9a), increasing the risk of scaling in the aforementioned areas, consistent with the higher EC values (Fig. 10a). In contrast, chalcedony SI ranged from −0.25 to >+0.75. The most critical zones are the eastern parts of the plain, with saturation increasing under lower temperature scenarios (−6 °C; Fig. 9b). In such cases, silica precipitation may act as a limiting factor, particularly under heating-mode operations. Measured pH values ranged from 5.6 to 8.4 (Fig. 10b). The main criticalities were identified in the southern portion of the study area and along the mouth of the Mesima river, where values frequently exceeding 8 may trigger phase precipitation processes governed by pH-dependent equilibria [50].

Concerning minor constituents, concentrations of Fe and Mn in the sampled waters were also considered, since they are indicative of possible oxide dissolution that could lead to further criticality in terms of release into solution of elements like As and other constituents with similar behaviour. Manganese shows great variability, with values

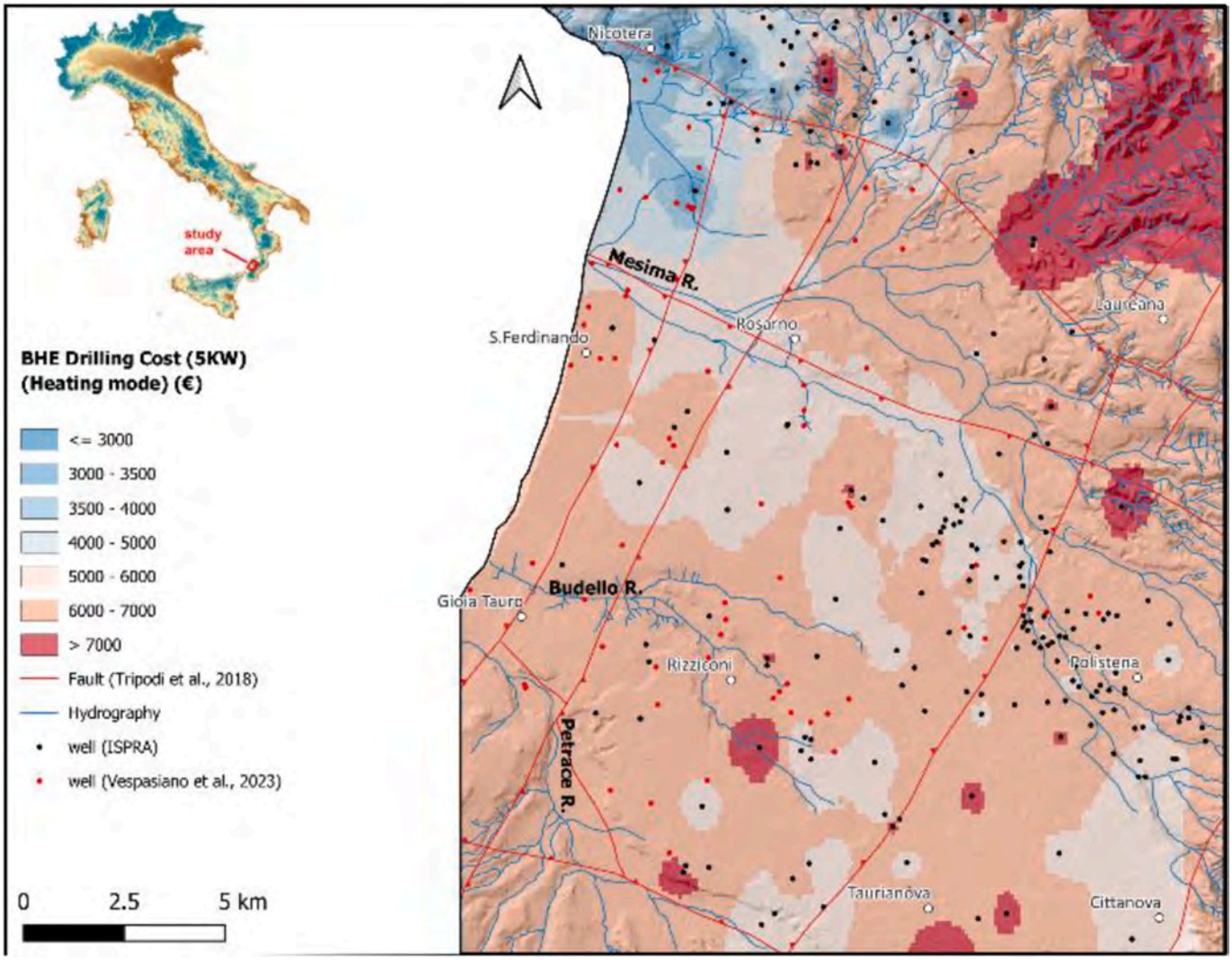

Fig. 6. Map of estimated drilling cost for the BHE realization (heating mode).

ranging from 0.6 to 2240 μg/L (Fig. 11a). The lowest values are found in the south-eastern area, while the highest in the north-eastern sector, probably due to the presence of Mn oxides in the crystalline basement and associated sedimentary infill of the plain [19]. Akin considerations can be made for Fe concentrations (Fig. 11b), highly variable (range: 8.2 and 4363 μg/L) and sharing a similar spatial correlation with Mn.

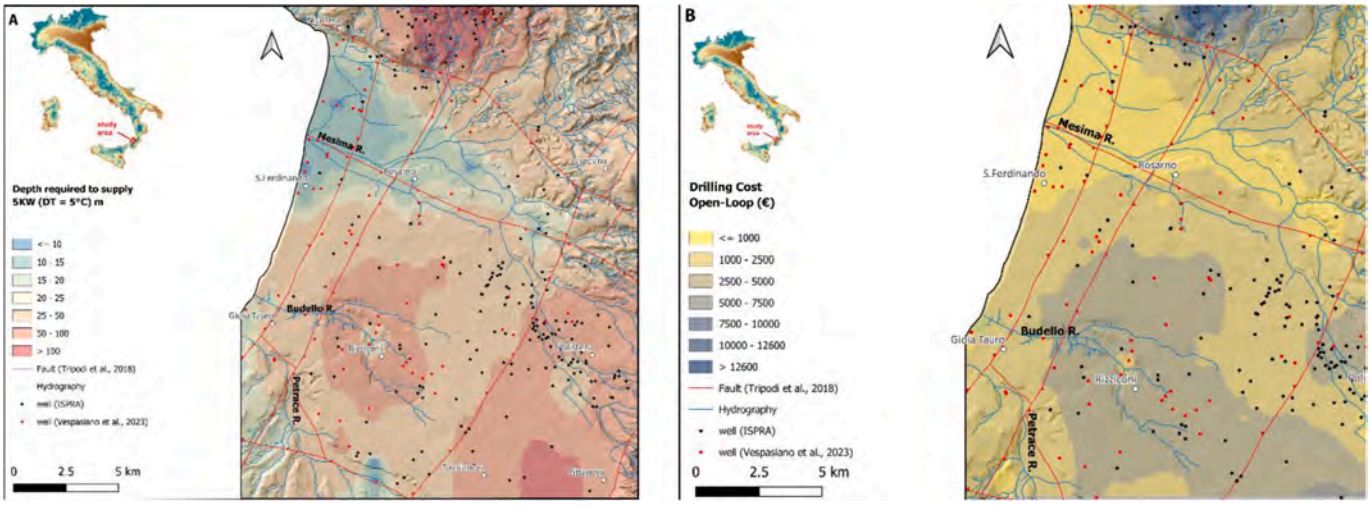

Fig. 7. (a) Map of the excavation depth required for the installation of GWHE systems to supply 5 kW of thermal energy and a ΔT of 6 °C and (b) Map of the estimated drilling cost for the GWHE realization.

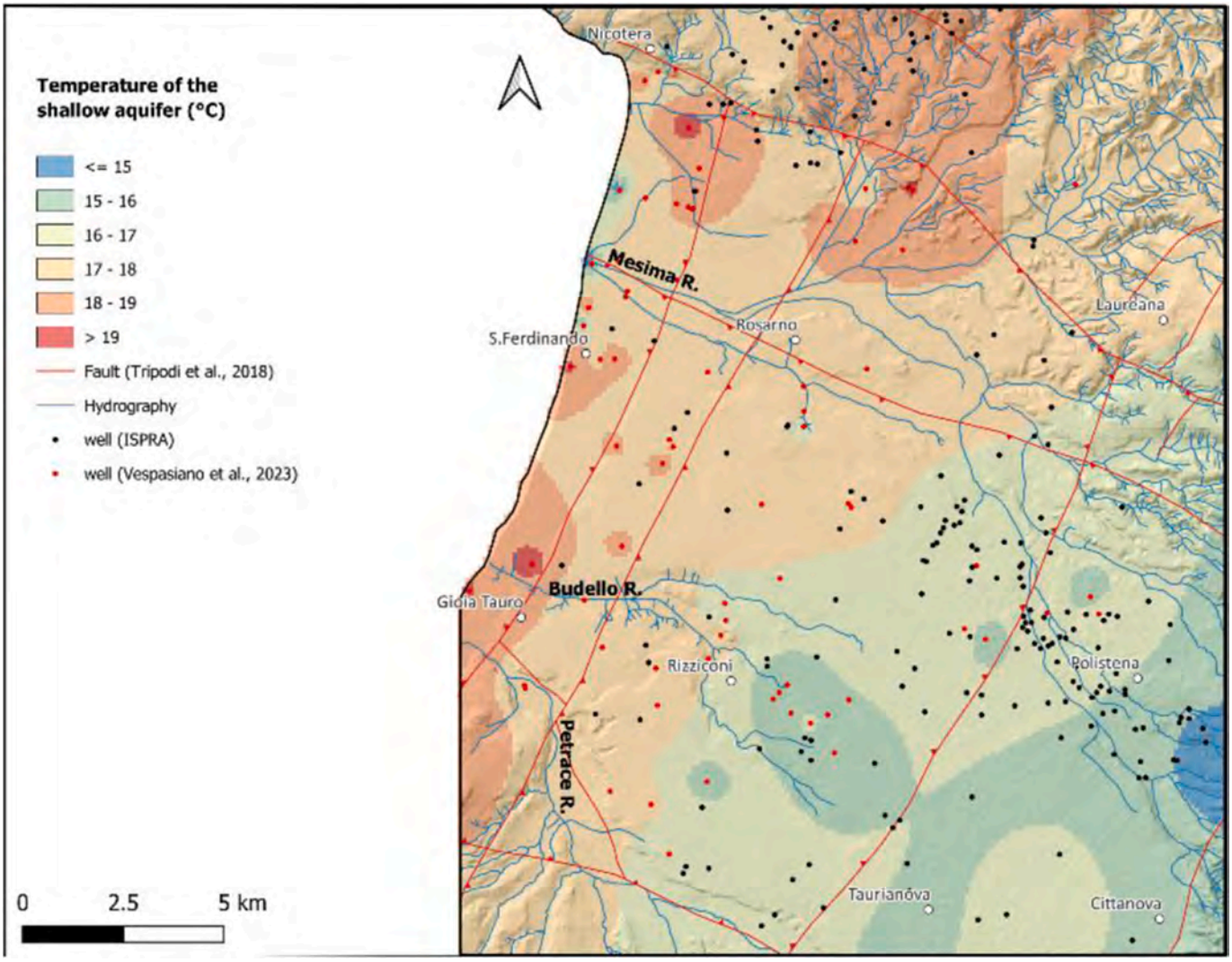

Fig. 8. Temperature distribution map of the shallow aquifer of the Gioia Tauro plain.

4.3.2. GPVI – index for estimating heat exchange potential for open-loop systems

The GPVI values (Table S4; [38]) were processed to generate the spatial distribution map (Fig. 12). Due to high subsurface K and shallow water tables, most of the plain exhibits favourable conditions for open-loop system development. Exceptions are found in the northeast sector and at the mouths of the Mesima and Budello rivers. Although these areas exhibit suitable values in terms of drilling depth and soil K, they also present significant physico-chemical limitations. Particularly, the northern sector and the Budello river mouth, are characterized by the highest groundwater temperatures, elevated salinity, and pronounced calcite oversaturation, conditions that could decrease open-loop system performance and promote bacterial proliferation. Also the Mesima river mouth shows relatively high salinity, elevated pH value and oversaturation with respect to calcite. All three critical areas are further distinguished by trace element concentrations (mainly Fe and Mn), far above the thresholds set by current regulations (Fig. 11).

Likewise to what assessed for the Q_{BHE}, we realized a comparison between the spatial distributions of the GPVI and population (Table 4). The GPVI was divided for simplicity into four conditions: (i) optimal (<2); (ii) very good (2<GPVI<4); (iii) boundary-to-likely unfavourable (4<GPVI<6); (iv) Unfavourable-to-very unfavourable (>6). The analysis shows that 47,130 persons live in very good conditions for implementing an open-loop system, while and 3643 persons live in boundary-to-likely unfavourable conditions. No people live in areas falling within high and low GPVI classes.

5. Conclusions and future outlooks

This study provides an integrated assessment of the shallow ground heat exchange potential of the Gioia Tauro plain, combining geological, hydrogeological, thermophysical, and geochemical data to evaluate the feasibility of Ground Source Heat Exchanger. The G.POT method identified the north-western sector as the most suitable area for closed-loop systems, offering high thermal yields and relatively low drilling costs, whereas the eastern sector shows lower potential due to the presence of unsaturated soils with low thermal conductivity. For open-loop systems, suitability is mainly controlled by the depth and hydrodynamic properties of the aquifer, with the central and coastal areas showing the most relevant conditions.

Geochemical analyses indicate that water composition does not significantly enhance corrosive processes, although localized scaling issues may occur. Calcite oversaturation is more pronounced in the northern and southwestern sectors and increases with temperature, while chalcedony is generally oversaturated, especially at lower groundwater temperatures. The potential for open-loop systems was further investigated by applying a new index (GPVI) that allows all required subsurface characteristics to be evaluated simultaneously. Its

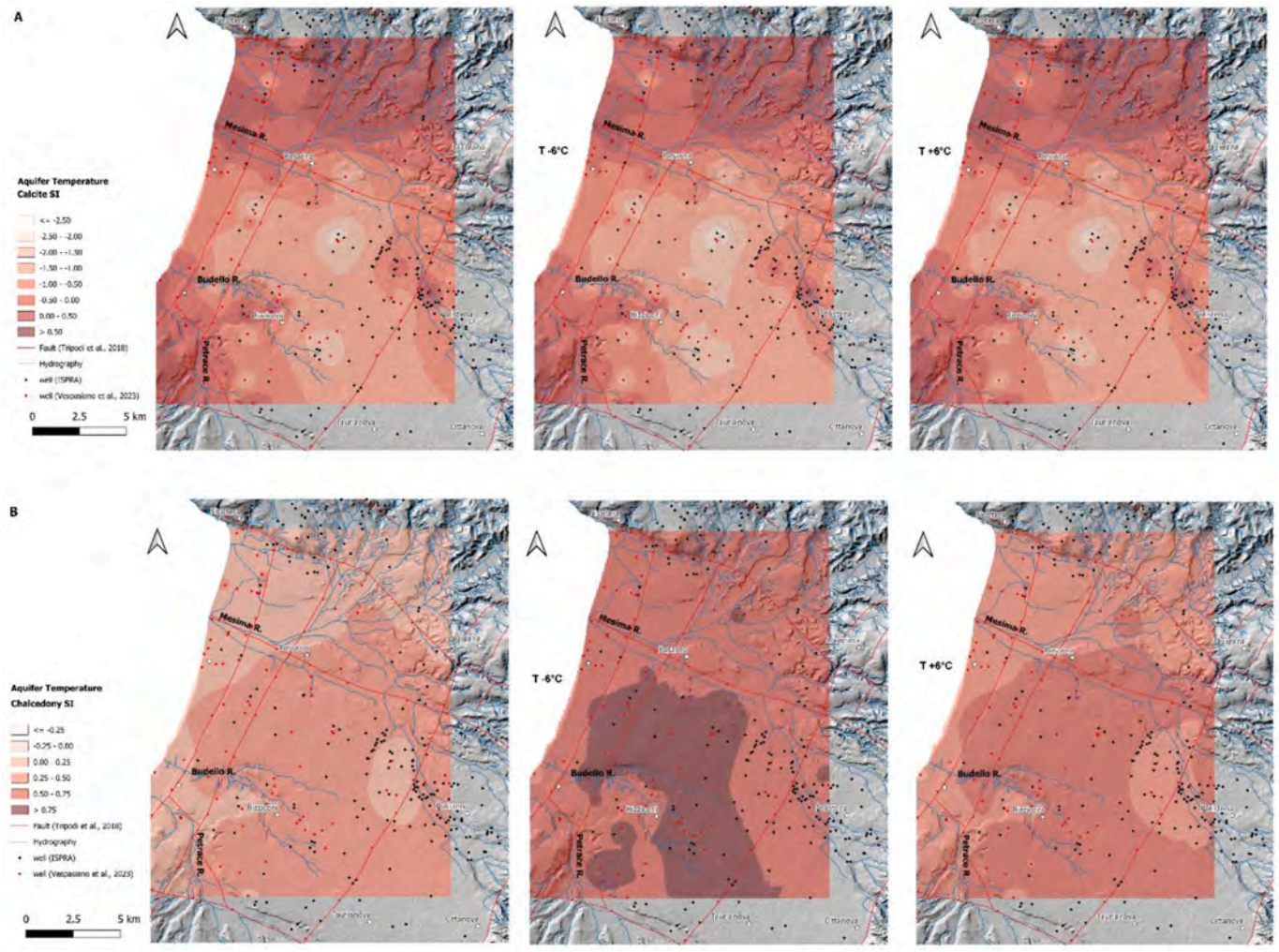

Fig. 9. Saturation index maps of (a) calcite and (b) chalcedony. For each phase, SI is reported, calculated for standard conditions (measured aquifer temperature) and ΔT of ±6 °C.

application, integrating aquifer depth, hydraulic conductivity, temperature, and water chemistry, confirms that most of the plain is suitable for open-loop installations. Critical conditions are limited to the northern sector and the Mesima and Budello river mouths, where high salinity, elevated temperatures, calcite oversaturation, and high Fe and Mn concentrations may reduce system efficiency and increase technical

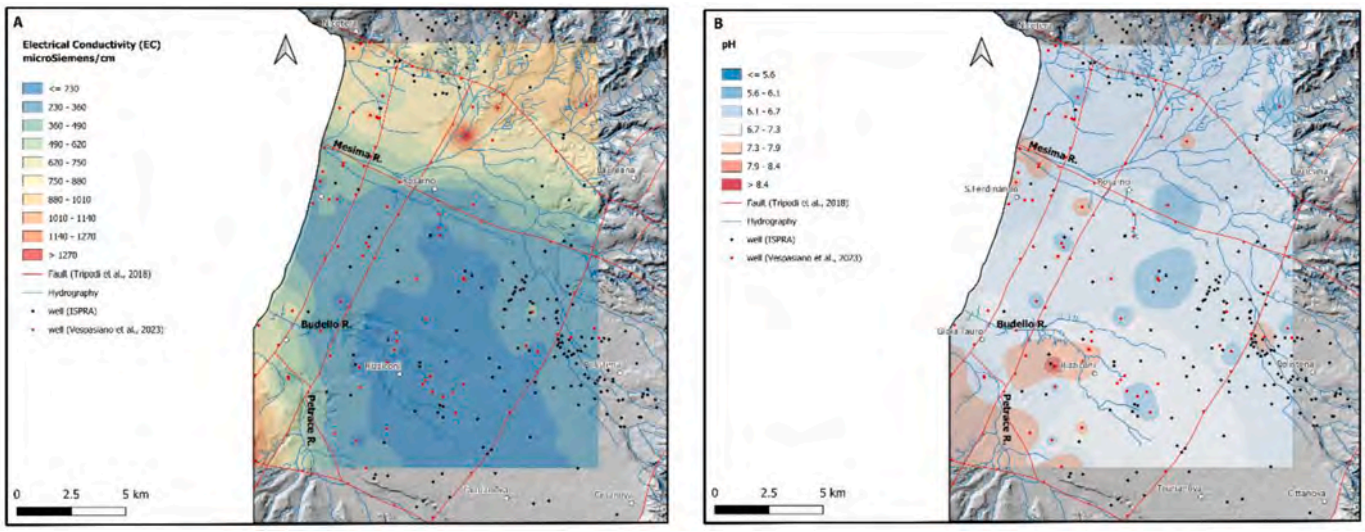

Fig. 10. Distribution maps of (a) electrical conductivity (EC in μS/cm) and (b) pH values of the shallow aquifer of the Gioia Tauro plain.

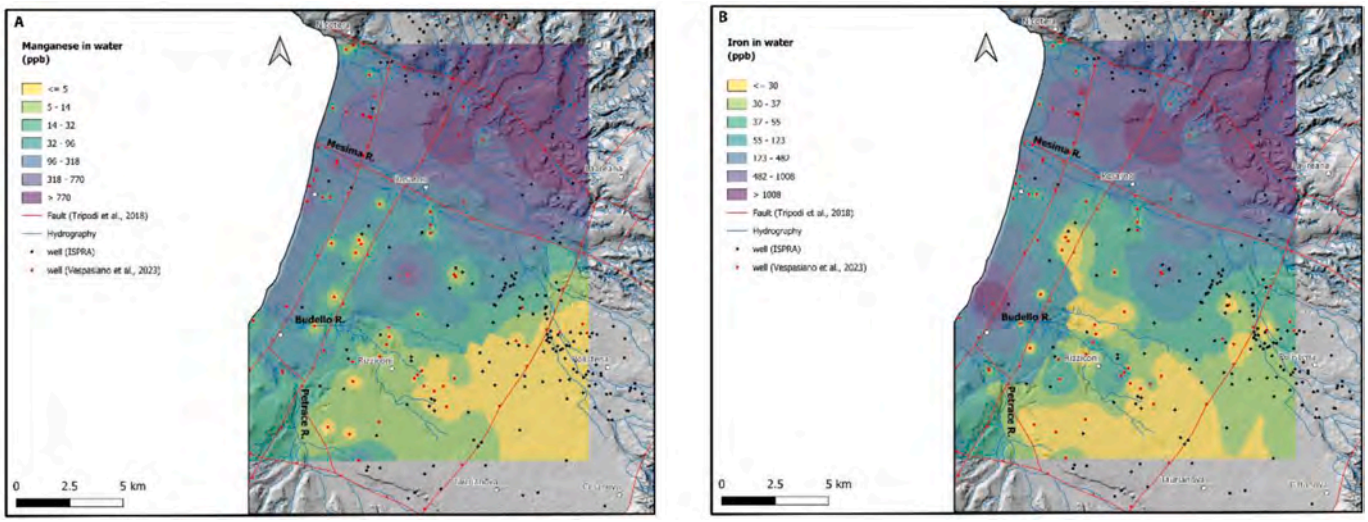

Fig. 11. Concentration map of (a) Mn and (b) Fe in the shallow water of the Gioia Tauro plain.

constraints. These findings underline the importance of a spatially integrated approach to shallow geothermal resource assessment, able to identifying areas of opportunity and facing technical and environmental challenges. This methodology can be adapted to other regions, supporting sustainable energy transition strategies at the local scale. The next challenges will focus on enhancing the GPVI to improve its

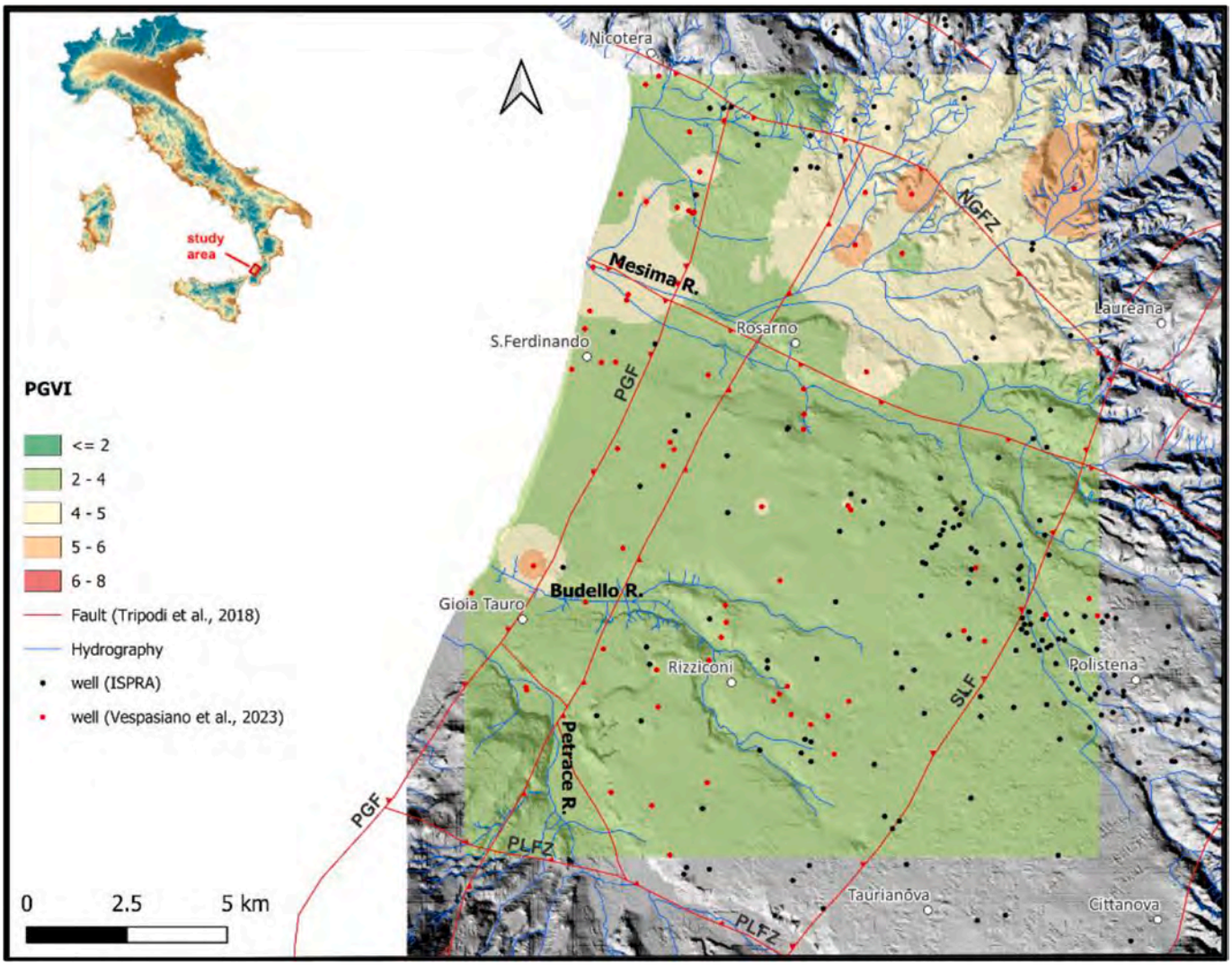

Fig. 12. Distribution map of the GPVI calculated for the study area.

Table 4
Comparison between the GPVI and the population living in the study area.

GPVI	Condition	Population (n. of inhabitants)
<2	Optimal	0
2 – 4	Very good	47,130
4 – 6	Boundary-to-likely unfavourable	3643
>6	Unfavourable-to-very unfavourable	0

adaptability in complex geological settings. Additionally, this method will be applied in other regions where monitoring active ground heat exchange systems may help refine the calibration of the methodology.

CRediT authorship contribution statement

Giovanni Vespasiano: Writing – review & editing, Writing – original draft, Visualization, Supervision, Project administration, Methodology, Investigation, Formal analysis, Data curation, Conceptualization. **Marco Taussi:** Writing – review & editing, Writing – original draft, Validation, Methodology, Investigation, Data curation, Conceptualization. **Luigi Russo:** Writing – review & editing, Writing – original draft, Visualization, Investigation, Formal analysis, Data curation. **Giuseppe Cianflone:** Writing – review & editing, Writing – original draft, Validation, Methodology, Investigation, Data curation, Conceptualization. **Lorenzo Chemeri:** Writing – original draft, Methodology, Investigation, Data curation. **Ilaria Fuoco:** Writing – review & editing, Writing – original draft, Visualization, Investigation, Formal analysis, Data curation. **Andrea Bloise:** Writing – review & editing, Writing – original draft, Validation. **Mauro F. La Russa:** Writing – review & editing, Validation. **Rocco Dominici:** Writing – review & editing, Validation. **Stefania Venturi:** Writing – review & editing, Methodology, Investigation, Data curation. **Jacopo Cabassi:** Writing – review & editing, Methodology, Investigation, Data curation. **Rosanna De Rosa:** Writing – review & editing, Validation, Funding acquisition. **Adriano Guido:** Writing – review & editing, Validation. **Alberto Renzulli:** Writing – review & editing, Validation. **Federico Ciniglia:** Writing – review & editing, Writing – original draft, Visualization, Investigation, Formal analysis, Data curation. **Carmine Apollaro:** Writing – review & editing, Writing – original draft, Validation, Methodology, Investigation, Funding acquisition, Data curation, Conceptualization.

Declaration of competing interest

The authors declare that they have no known competing financial interests or personal relationships that could have appeared to influence the work reported in this paper.

Acknowledgements

This work was funded by the Next Generation EU - Italian NRRP, Mission 4, Component 2, Investment 1.5, call for the creation and strengthening of 'Innovation Ecosystems', building 'Territorial R&D Leaders' (Directorial Decree n. 2021/3277) - project Tech4You - Technologies for climate change adaptation and quality of life improvement, n. ECS0000009 and by PRIN 2022 PNRR-Thermal model of Aeolian Islands for new perspectives of sustainable exploitation of geothermal resources, CUP H53D23011420001. This work reflects only the authors' views and opinions, neither the Ministry for University and Research nor the European Commission can be considered responsible for them. The authors want to thank the two anonymous reviewers that helped to improve this work, and the Editors for the comments and editorial handling.

Appendix A. Supplementary data

Supplementary data to this article can be found online at https://doi.org/10.1016/j.renene.2026.125807.

Data availability

The data used in this work are available in Vespasiano et al. [38] through Mendeley Data at: https://data.mendeley.com/preview/k76ysjzvr5?a=b2b16ef5-0f6b-43d8-9e5a-15e14619113f.

References

[1] J.W. Lund, A.N. Toth, Direct utilization of geothermal energy 2020 worldwide review, Geothermics 90 (2021) 101915.
[2] L. Marini, G. Vespasiano, R. De Rosa, M. Viccaro, C. Principe, A. Bloise, I. Fuoco, M. Lelli, M.F. La Russa, C.G. Caruso, A. Gattuso, G. Lazzaro, M. Longo, A. Guido, F. Muto, L. Russo, F. Ciniglia, A.A. Tsegaye, C. Apollaro, The geothermal resources of Vulcano Island (Aeolian archipelago, Italy), Renew. Energy 253 (2025) 123622, https://doi.org/10.1016/j.renene.2025.123622.
[3] Vespasiano G., Floridia G., Giuffrida M., Viccaro M., Bloise A., De Rosa R., Cacace M., Fuoco I., La Russa M., Muto F., Dominici R., Russo L., Cipriani M., Guido A., Maruca G., Apollaro C., 3D lithospheric thermal model of the Calabria region (Southern Italy): a supporting tool for new exploration campaigns for geothermal resources. Geothermics, 136, 103604.
[4] D. Viesi, A. Galgaro, P. Visintainer, L. Crema, GIS-supported evaluation and mapping of the geo-exchange potential for vertical closed-loop systems in an alpine valley, the case study of adige valley (Italy), Geothermics 71 (2018) 70–87, https://doi.org/10.1016/j.geothermics.2017.08.008.
[5] G. Florides, S. Kalogirou, Ground heat exchangers—A review of systems, models and applications, Renew. Energy 32 (15) (2007) 2461–2478, https://doi.org/10.1016/j.renene.2006.12.014.
[6] A.M. Omer, Ground-source heat pumps systems and applications, Renew. Sustain. Energy Rev. 12 (2008) 344–371.
[7] C. Lohse, Environmental impact by hydrogeothermal energy generation in low-enthalpy regions, Renew. Energy 128 (2018) 509–519, https://doi.org/10.1016/j.renene.2017.06.030.
[8] M. Muñoz, P. Garat, V. Flores-Aqueveque, G. Vargas, S. Rebolledo, S. Sepúlveda, L. Daniele, D. Morata, M.Á. Parada, Estimating low-enthalpy geothermal energy potential for district heating in Santiago basin–Chile (33.5° S), Renew. Energy 76 (2015) 186–195, https://doi.org/10.1016/j.renene.2014.11.019.
[9] A. Casasso, R. Sethi, Assessment and mapping of the shallow geothermal potential in the province of Cuneo (Piedmont, NW Italy), Renew. Energy 102 (2017) 306–315, https://doi.org/10.1016/j.renene.2016.10.045.
[10] S. Lo Russo, M.V. Civita, Open-loop groundwater heat pumps development for large buildings: a case study, Geothermics 38 (3) (2009) 335–345, https://doi.org/10.1016/j.geothermics.2008.12.009.
[11] F. Piscaglia, A. Blasi, S. Del Moro, F. Polonara, A. Arteconi, L. Zanarelli, A. Renzulli, Monitoring of a vertical borehole ground-coupled heat pump system: a case study from a marly-limestone heat reservoir (Urbino, Central Italy), Geothermics 62 (2016) 61–69, https://doi.org/10.1016/j.geothermics.2016.02.008.
[12] A. Manzella, D. Serra, G. Cesari, E. Bargiacchi, M. Cei, P. Cerutti, P. Conti, G. Giudetti, M. Lupi, M. Vaccaro, Geothermal energy use, country update for Italy. European Geothermal Congress 2019, Den Haag, The Netherlands, 2019, pp. 11–14. June 2019.
[13] A. Galgaro, E. Di Sipio, G. Teza, E. Destro, M. De Carli, S. Chiesa, A. Zarrella, G. Emmi, A. Manzella, Empirical modeling of maps of geo-exchange potential for shallow geothermal energy at regional scale, Geothermics 57 (2015) 173–184, https://doi.org/10.1016/j.geothermics.2015.06.017.
[14] A. Ramos-Escudero, M.S. García-Cascales, J.F. Urchueguía, Evaluation of the shallow geothermal potential for heating and cooling and its integration in the socioeconomic environment: a case study in the region of Murcia, Spain, Energies 14 (18) (2021) 5740, https://doi.org/10.3390/en14185740.
[15] A. Casasso, R. Sethi, G. POT: a quantitative method for the assessment and mapping of the shallow geothermal potential, Energy 106 (2016) 765–773, https://doi.org/10.1016/j.energy.2016.03.091.
[16] C. Apollaro, G. Vespasiano, I. Fuoco, M. Taussi, R. De Rosa, M.F. La Russa, A. Guido, D. Di Curzio, A. Renzulli, L. Russo, F. Ciniglia, F. D'Amico, M. Cipriani, G. Maruca, G. Virgili, A. Bloise, Impact and evaluation of potential implications of coastal plains on soil greenhouse gas emissions: insights from the sibari coastal plain (Calabria, Southern Italy), Sci. Total Environ. 964 (2025) 178611, https://doi.org/10.1016/j.scitotenv.2025.178611.
[17] C. Monaco, L. Tortorici, Active faulting in the Calabrian arc and eastern Sicily, J. Geodyn. 29 (3–5) (2000) 407–424.
[18] G. Cianflone, G. Vespasiano, C. Tolomei, R. De Rosa, R. Dominici, C. Apollaro, K. Walraevens, M. Polemio, Different ground subsidence contributions revealed by integrated discussion of Sentinel-1 datasets, well discharge, stratigraphical and geo morphological data: the case of the Gioia Tauro Coastal plain (Southern Italy), Sustainability 2926 (2022), https://doi.org/10.3390/su14052926.
[19] G. Vespasiano, G. Cianflone, L. Marini, R. De Rosa, M. Polemio, K. Walraevens, O. Vaselli, L. Pizzino, D. Cinti, F. Capecchiacci, D. Barca, R. Dominci, C. Apollaro, Hydrogeochemical and isotopic characterization of the Gioia Tauro coastal plain (Calabria-southern Italy): a multidisciplinary approach for a focused management of vulnerable strategic systems, Sci. Total Environ. 862 (2023) 160694, https://doi.org/10.1016/j.scitotenv.2022.160694.

[20] R. Cirrincione, E. Fazio, P. Fiannacca, G. Ortolano, A. Pezzino, R. Punturo, The Calabria-Peloritani Orogen, a composite terrane in central Mediterranean; its overall architecture and geodynamic significance for a pre-alpine scenario around the Tethyan basin, Period. Mineral. 84 (3B) (2015) 701–749, https://doi.org/10.2451/2015PM0446.
[21] E. Jacques, C. Monaco, P. Tapponnier, L. Tortorici, T. Winter, Faulting and earthquake triggering during the 1783 Calabria seismic sequence, Geophys. J. Int. 147 (2001) 499–516, https://doi.org/10.1046/j.0956-540x.2001.01518.x.
[22] V. Tripodi, F. Muto, F. Brutto, F. Perri, S. Critelli, Neogene-quaternary evolution of the forearc and backarc regions between the Serre and aspromonte massifs, Calabria (southern Italy), Mar. Petrol. Geol. 95 (2018) 328–343, https://doi.org/10.1016/j.marpetgeo.2018.03.028.
[23] G. Cianflone, G. Vespasiano, R. De Rosa, R. Dominici, C. Apollaro, O. Vaselli, L. Pizzino, C. Tolomei, F. Capecchiacci, M. Polemio, Hydrostratigraphic framework and physicochemical status of groundwater in the Gioia Tauro coastal plain (Calabria— Southern Italy), Water 13 (2021) 3279, https://doi.org/10.3390/w13223279.
[24] ISPRA, Foglio 590-Taurianova. Carta geologica D'Italia Alla Scala 1:50.000, Istituto Superiore per la Protezione e la Ricerca Ambientale, Roma, 2016.
[25] C. Apollaro, V. Tripodi, G. Vespasiano, R. De Rosa, E. Dotsika, I. Fuoco, S. Critelli, F. Muto, Chemical, isotopic and geotectonic relations of the warm and cold waters of the Galatro and Antonimina thermal areas, southern Calabria, Italy, Mar. Petrol. Geol. 109 (2019) 469–483, https://doi.org/10.1016/j.marpetgeo.2019.06.020.
[26] C. Apollaro, A. Buccianti, G. Vespasiano, M. Vardè, I. Fuoco, D. Barca, A. Bloise, D. Miriello, F. Cofone, A. Servidio, Rosa R. De, Comparative geochemical study between the tap waters and the bottled mineral waters in Calabria (southern Italy) by compositional data analysis (CoDA) developments, Appl. Geochem. 107 (2019) 19–33, https://doi.org/10.1016/j.apgeochem.2019.05.011.
[27] ISPRA, National archives of subsurface investigations L.464/84. https://www.isprambiente.gov.it/it/attivita/suolo-e-territorio/archivio-dei-sondaggi-ex-lege-464-84, 2017.
[28] J. Ondreka, M.I. Rüsgen, I. Stober, K. Czurda, GIS-supported mapping of shallow geothermal potential of representative areas in south-western Germany—possibilities and limitations, Renew. Energy 32 (13) (2007) 2186–2200, https://doi.org/10.1016/j.renene.2006.11.009.
[29] M. Taussi, W. Borghi, M. Gliaschera, A. Renzulli, Defining the shallow geothermal heat-exchange potential for a lower fluvial plain of the central apennines: the metauro valley (Marche region, Italy), Energies 14 (3) (2021) 768, https://doi.org/10.3390/en14030768.
[30] M. Di Pierdomenico, M. Taussi, A. Galgaro, G. Dalla Santa, M. Maggini, A. Renzulli, Shallow geothermal potential and numerical modelling of the geo-exchange for a sustainable post-earthquake building reconstruction (Potenza river valley, Marche region, Central Italy), Geothermics 119 (2024) 102954, https://doi.org/10.1016/j.geothermics.2024.102954.
[31] G. Vespasiano, G. Cianflone, M. Taussi, R. De Rosa, R. Dominci, C. Apollaro, Shallow geothermal potential of the sant'eufemia plain (South Italy) for heating and cooling systems, a potential solution in a climate-changing society, Geosciences 13 (4) (2023) 110, https://doi.org/10.3390/geosciences13040110, 2023.
[32] TCSM, Technical commission for seismic microzonation. https://www.centromicrozonazionesismica.it/en/tools/guidelines-sm/, 2018.
[33] M. Verdoya, C. Pacetti, P. Chiozzi, C. Invernizzi, Thermophysical parameters from laboratory measurements and in-situ tests in borehole heat exchangers, Appl. Therm. Eng. 144 (2018) 711–720.
[34] E. Di Sipio, A. Galgaro, E. Destro, G. Teza, S. Chiesa, A. Giaretta, A. Manzella, Subsurface thermal conductivity assessment in Calabria (southern Italy): a regional case study, Environ. Earth Sci. 72 (2014) 1383–1401, https://doi.org/10.1007/s12665-014-3277-7.
[35] G. Dalla Santa, A. Galgaro, R. Sassi, M. Cultrera, P. Scotton, J. Mueller, D. Bertermann, D. Mendrinos, R. Pasquali, R. Perego, S. Pera, E. Di Sipio, G. Cassiani, M. De Carli, A. Bernardi, An updated ground thermal properties database for GSHP applications, Geothermics 85 (2020) 101758, https://doi.org/10.1016/j.geothermics.2019.101758.
[36] VDI 4640, Thermische Nutzung Des Untergrundes, Erdgekoppelte Wärmepumpenanlagen. VDI-Richtlinien 4640, Bd. Blatt 2. Aufl, Beuth Verlag, Berlin, 2001.
[37] J.M. Andújar Márquez, M.Á. Martínez Bohórquez, S. Gómez Melgar, Ground thermal diffusivity calculation by direct soil temperature measurement. Application to very low enthalpy geothermal energy systems, Sensors 16 (3) (2016) 306, https://doi.org/10.3390/s16030306.
[38] G. Vespasiano, M. Taussi, L. Russo, G. Cianflone, L. Chemeri, I. Fuoco, A. Bloise, M. La Russa, R. Dominici, S. Venturi, J. Cabassi, R. De Rosa, A. Guido, A. Renzulli, F. Ciniglia, C. Apollaro, Data for: integrating classical methods and a new viability index to assess shallow ground heat exchange potential: application to the Gioia Tauro coastal plain (Calabria, Southern Italy)", Mendeley Data V1 (2026) https://doi.org/10.17632/k76ysjzvr5.1. https://data.mendeley.com/preview/k76ysjzvr5?a=b2b16ef5-0f6b-43d8-9e5a-15e14619113f.
[39] S. Adrinek, M. Janža, M. Brenčič, Impact of open-loop systems on groundwater temperature in NE Slovenia, Sustainability 15 (18) (2023) 13797, https://doi.org/10.3390/su151813797.
[40] J. Logan, Estimating transmissibility from routine production tests of water wells, Groundwater 2 (1) (1964) 35–37, https://doi.org/10.1111/j.1745-6584.1964.tb01744.x.
[41] H. Brielmann, C. Griebler, S.I. Schmidt, R. Michel, T. Lueders, Effects of thermal energy discharge on shallow groundwater ecosystems, FEMS Microbiol. Ecol. 68 (3) (2009) 273–286, https://doi.org/10.1111/j.1574-6941.2009.00674.x.
[42] A. García-Gil, J. Epting, E. Garrido, E. Vázquez-Suñé, J.M. Lázaro, J.A. Sánchez Navarro, P. Huggenberger, M.A. Marazuela Calvo, A city scale study on the effects of intensive groundwater heat pump systems on heavy metal contents in groundwater, Sci. Total Environ. 572 (2016) 1047–1058, https://doi.org/10.1016/j.scitotenv.2016.08.010.
[43] S. Bezelgues-Courtade, J.C. Martin, S. Schomburgk, P. Monnot, D. Nguyen, M. Le Brun, A. Desplan, Geothermal potential of shallow aquifers: decision-aid tool for heat-pump installation, in: World Geothermal Congress 2010, 2010, p. 9.
[44] D.L. Parkhurst, C.A.J. Appelo, Description of Input and Examples for PHREEQC Version 3—A Computer Program for Speciation, batch-reaction, one-dimensional Transport, and Inverse Geochemical Calculations, U.S. Geological Survey Techniques and Methods, 2013, p. 497, book 6, chap. A43, available only at, https://pubs.usgs.gov/tm/06/a43/.
[45] L. Chemeri, J. Cabassi, M. Taussi, S. Venturi, Development and testing of a new flexible, easily and widely applicable chemical water quality index (CWQI), J. Environ. Manag. 348 (2023) 119383.
[46] L.A. Richards, Diagnosis and improvement of saline alkali soils, in: Agriculture, 160. Handbook 60, Department of Agriculture, Washington, DC, USA, 1954.
[47] A. Casasso, R. Sethi, Assessment and minimization of potential environmental impacts of ground source heat pump (GSHP) systems, Water 11 (8) (2019) 1573, https://doi.org/10.3390/w11081573.
[48] C.W. Fetter, Applied Hydrogeology, Pearson, London, UK, 2014.
[49] EU Directive 2020/2184 of the European Parliament and of the Council of 16 December 2020 on the quality of water intended for human consumption 2020, p. 1 (recast) (Text with EEA relevance) (OJ L 435 23.12., ELI: http://data.europa.eu/eli/dir/2020/2184/oj).
[50] C. Appelo, D. Postma, Geochemistry, Groundwater and Pollution, second ed., Balkema, Rotterdam, 2005 https://doi.org/10.1201/9781439833544.